DEPARTMENT OF DEFENCE
DEFENCE SCIENCE & TECHNOLOGY ORGANISATION
DSTO

Prediction of Buffet Loads Using Artificial Neural Networks

Oleg Levinski

DSTO-RR-0218

Prediction of Buffet Loads Using Artificial Neural Networks

Oleg Levinski

Airframes and Engines Division
Aeronautical and Maritime Research Laboratory

DSTO-RR-0218

ABSTRACT

The use of artificial neural networks (ANN) for predicting the empennage buffet pressures as a function of aircraft state has been investigated. The buffet loads prediction method which is developed depends on experimental data to train the ANN algorithm and is able to expand its knowledge base with additional data. The study confirmed that neural networks have a great potential as a method for modelling buffet data. The ability of neural networks to accurately predict magnitude and spectral content of unsteady buffet pressures was demonstrated. Based on the ANN methodology investigated, a buffet prediction system can be developed to characterise the F/A-18 vertical tail buffet environment at different flight conditions. It will allow better understanding and more efficient alleviation of the empennage buffeting problem .

RELEASE LIMITATION

Approved for public release

DEPARTMENT OF DEFENCE
DEFENCE SCIENCE & TECHNOLOGY ORGANISATION
DSTO

Published by

DSTO Aeronautical and Maritime Research Laboratory
506 Lorimer St
Fishermans Bend, Victoria 3207 Australia

Telephone: (03) 9626 7000
Fax: (03) 9626 7999

AR-012-019
September 2001

APPROVED FOR PUBLIC RELEASE

Prediction of Buffet Loads Using Artificial Neural Networks

Executive Summary

The F/A-18 fighter aircraft experiences random fluctuating pressures on its empennage surfaces caused by impingement of burst LEX vortices during critical high angle of attack manoeuvres. This severe buffet environment shortens structural fatigue life and causes premature structural failures. Accurate prediction of random pressure fluctuations on a vertical tail is quite difficult due to complexities in the interaction between the highly turbulent flow field behind burst LEX vortices and empennage structure in different flight regimes. Despite progress in our ability to predict the empennage buffet made during the last decade, more accurate and robust buffet prediction methods must be developed to support fleet management decisions.

This work investigates the feasibility of using Artificial Neural Networks (ANN) for predicting the empennage buffet pressures as a function of flight conditions. The method is dependent on the availability of experimental data to train the ANN algorithm and is able to expand its knowledge base with additional data. Full scale F/A-18 tail buffet test in the 80ft X 120ft test section of the NASA Ames National Full-Scale Aerodynamics Complex provided the initial database for the development and assessment of an ANN-based buffet load prediction method.

The study revealed that artificial neural networks have a great potential as a method for modelling the complex nonlinear relationships inherent in buffet data. Initial assessments indicated that neural networks are able to accurately predict RMS values and frequency content of unsteady buffet pressures. The ANNs have the ability to extract the essential features from many input combinations to produce an accurate output and generalise well for new conditions by detecting features of the inputs that have been learned to be significant.

Based on the ANN methodology investigated, a buffet prediction system can be developed to provide detailed information about the F/A-18 vertical tail buffet environments through the use of additional experimental and flight test data. It will allow for better understanding of empennage buffeting problems and can be used in fatigue usage monitoring systems for fleet aircraft. Results of the work contribute to DSTO's existing body of knowledge on empennage buffet and can assist in the F/A-18 International Follow On Structural Test Project (IFOSTP) fatigue test on the aft fuselage and empennage.

Authors

Dr Oleg Levinski
Airframes and Engines Division

Oleg Levinski completed his Bachelor of Science in Aeronautical Engineering (Honours) at the Joukowski Institute of Aviation, Ukraine, in 1985. He has worked for several years with aircraft design and production organisations. He has been awarded 5 patents in the field of aeronautical/mechanical engineering and has published a number of papers. He completed his Doctorate at the University of Melbourne in 1997 and joined the Aeronautical and Maritime Research Laboratory the same year. He is currently a Research Scientist in the Airframes and Engines Division and his area of research is computational unsteady aerodynamics, structural dynamics and aeroelasticity.

Contents

1. Introduction

The unsteady pressures acting on the aircraft lifting surfaces, referred to as buffet, are broadband random fluctuations having predominant frequencies associated with the primary aerodynamic characteristics of the aircraft. Twin-tail fighter aircraft such as F/A-18 have proven to be especially susceptible to empennage buffet at high angles of attack. The vortices emanating from the wing root leading edge extensions (LEXs) tend to burst producing highly energetic swirling flow, which convects downstream and impinges upon the vertical tails and horizontal stabilators. The turbulent airflow following a burst LEX vortex excites the tail surfaces and large oscillatory structural responses result at the low order resonant frequencies of the tail. After prolonged exposure to this dynamic environment, the tail structure begins to fatigue and repairs must be initiated. The maintenance costs and aircraft down-time associated with these repairs are often quite high.

The accurate prediction of the random pressure environment on a vertical tail is difficult due to the complexity of the interaction between the aircraft state, burst vortex flowfield and empennage structure, see Mabey [1], Lee & Brown [2]. During the past decades, intensive theoretical and experimental investigations of the mechanism of leading edge vortex breakdown improved our understanding of this complex phenomenon. Despite some progress in the prediction of LEX vortex breakdown, the underlying physical process governing the breakdown and how it causes tail buffet are still among the most challenging fundamental research problems.

A number of sub-scale and full-scale experiments [2 - 6] on F/A-18 tail buffet, aircraft flight tests [7, 8], as well as numerical predictions [9, 10, 11] performed so far provide valuable information about buffet pressure distributions, dynamic response of the vertical tails and some details of the flowfield in the vertical tail region. These experiments and flight tests form a database of dynamic load environments, which can be utilised in order to develop an accurate and robust buffet prediction method.

The main objective of this study is to determine the feasibility of using Artificial Neural Networks (ANN) to characterise the unsteady buffet loads as a function of aircraft state using aerodynamic pressures measured on the twin tails of an F/A-18. The data were obtained from a full-scale F/A-18 tail buffet test at the NASA Ames Research Center where buffet pressures and the resulting structural vibrations of the vertical tails were obtained over a range of angles of attack and sideslip. It provided the initial information required for the development and assessment of an ANN-based buffet loads prediction method.

This work has been done as part of an effort to develop a buffet prediction system, which incorporates experimental and flight test data, computational unsteady aerodynamics and artificial neural networks and can be used to further improve the service life of fleet aircraft and reduce costly post-production repairs.

2. Full-Scale Tail Buffet Test

In 1991, the Aeronautical and Maritime Research Laboratory (AMRL) participated in tests of a full-scale F/A-18 aircraft in the 80ft X 120ft wind tunnel of the National Full-Scale Aerodynamic Complex at the NASA Ames Research Centre in Moffett Field, California. The wind tunnel test was part of NASA's High Alpha Technology Program, a cooperative research effort at NASA's Ames, Langley and Lewis Research Centers to improve the manoeuvrability of high performance military aircraft at very high angles of attack. It was conducted in an attempt to quantify the F/A-18 tail buffet loads and to provide data for use in the development of potential solutions to counter the twin tail buffet problem.

The main purpose of this test was to obtain further information on the unsteady excitation experienced by the vertical tails at high angle of attack, using unsteady surface pressure measurements, and on the tail response, using acceleration measurements of the tail structure. Buffet pressures and the resulting structural vibrations of the vertical tails were obtained over a range of angles of attack and sideslip. The information from the NASA tests was used to augment AMRL studies on vortex breakdown and to help define the loading spectrum for the F/A-18 International Follow On Structural Test Project (IFOSTP) fatigue test on aft fuselage and empennage.

2.1 Wind Tunnel

The 80ft X 120ft Wind Tunnel is part of the National Full-Scale Aerodynamic Complex (NFAC) located at NASA Ames Research Center. The NFAC can be configured as either a closed circuit wind tunnel with a 40ft X 80ft test section or an open circuit wind tunnel with an 80ft X 120ft test section, see Figure 1. The maximum dynamic pressure attainable in the 80ft X 120ft Wind Tunnel is 33 psf, providing a maximum velocity of approximately 100 knots. The maximum speed corresponds to a Reynolds number of 12.3×10^6 based on the F/A-18 wing's mean aerodynamic chord.

2.2 Test Article

Vertical tail buffet studies were conducted on a full-scale production F/A-18 fighter aircraft. The aircraft, supplied by the U.S. Navy, was from the first F/A-18 model A production block. The aircraft is 56.0 ft long and has a wingspan of 37.42 ft. The reference wing area is 400 ft^2 and the wing's mean aerodynamic chord is 11.52 ft. The leading edge flaps were fixed at a 33 deg. deflection angle and trailing edge flaps were fixed in their undeflected position. These flap deflections match the standard control law schedule for angles of attack greater than 26 deg. The rudders were fixed in their undeflected position throughout the test. The horizontal stabilators were actuated so

that their position was varied with angle of attack to match the trimmed stabilator positions of those on the High Angle-of-attack Research Vehicle (HARV) in steady, 1g flight conditions. The aircraft engines and avionics were removed prior to test. The aircraft was configured with flow-through inlets and the missile rails were left in place on the wing tips with no missiles attached.

The aircraft was supported in the wind tunnel test section by the three struts, as shown in Figure 2. Two main struts of fixed height were attached to the aircraft with two blade and clevis assemblies that replaced the main landing gear trunnions. The third strut, a large linear actuator that positioned the tail linearly to control the angle of attack, was connected to the aircraft by a cantilever structure attached to the engine mounts and to the arresting hook pivot. The three struts were mounted on a rotatable turntable in the floor of the wind tunnel that allowed placing the test article at various sideslip orientations.

The F/A-18 was tested over an angle of attack range of 18 to 50 degrees, a sideslip range of -15 to 15 degrees, and at wind speeds up to 100 knots. The test conditions for which pressures and accelerations were available are summarised in Table 1. The parameters listed include the static angle of attack and angle of sideslip for each run along with the use of the LEX fence. Here, a positive sideslip is nose left from the pilot's perspective. All of the runs presented in Table 1 were conducted at a free stream velocity of 168 ft/s. This corresponds to a dynamic pressure of approximately 33 psf and a Mach number of 0.15.

Table 1 Tail Buffet Test Conditions

Run #	LEX Fence	Alpha	Beta	Sweep Values
44	Off	30	Sweep	15, 10, 6, 4, 2, 0, -2, -4, -5, -10, -15
45	Off	Sweep	0	18, 20, 24, 26, 28, 30, 32, 35, 40, 45, 50
46	Off	40	Sweep	15, 10, 6, 4, 2, 0, -2, -4, -6, -10, -15
47	Off	25	Sweep	15, 10, 6, 4, 2, 0, -2, -4, -6, -10, -15
48	Off	35	Sweep	15, 10, 6, 4, 2, 0, -2, -4, -6, -10, -15
53	Off	45	Sweep	15, 10, 5, 2, 0, -2, -5, -10, -15
54	Off	50	Sweep	15, 10, 5, 2, 0, -2, -5, -10, -15
58	Off	Sweep	0	18, 20, 24, 26, 28, 30, 32, 34, 36, 38, 40, 42, 44, 46, 48, 50
61	On	30	Sweep	15, 10, 5, 2, 0, -2, -5, -10, -15
62	On	Sweep	0	18, 20, 24, 26, 28, 30, 32, 35, 40, 45, 50
63	On	25	Sweep	15, 10, 5, 2, 0, -2, -5, -10, -15
64	On	35	Sweep	15, 10, 5, 2, 0, -2, -5, -10, -15

2.3 Instrumentation

The F/A-18 tail buffet test instrumentation consisted of 32 pressure transducers, eight accelerometers, six strain gauges, and a surface temperature sensor. The pressure transducers were mounted on the surface of the port vertical tail in a four by four matrix on both the inboard and outboard surfaces, as shown in Figure 3. Each vertical tail and each horizontal stabilator had two accelerometers mounted at their tips near the leading and trailing edges. The strain gages were installed on the attachment stubs of both vertical tails and the temperature sensor was attached to the surface of the port vertical tail.

Data were sampled at a rate of 512 Hz per channel for a period of 32 seconds. To eliminate concerns about attenuation in pressure tubing and to simplify transducer installation, absolute pressure transducers, that did not have reference pressure lines, were installed on the tail surfaces. Transducers were mounted in fairings to minimise disturbances to the flow. The signals from the pressure transducers were AC coupled to eliminate the large DC offset due to atmospheric pressure and thereby allowed greater signal gain for increased resolution of the unsteady pressures measured.

3. Data Reduction

The F/A-18 tail buffet test data were provided to AMRL under the guidelines of The Technical Cooperation Program (TTCP), Technical Panel HTP-5, Manoeuvring Aerodynamics. It included all dynamic data from runs 44, 45, 46, 47, 48, 53, 54, 58, 61, 62, 63 and 64, as shown in Table 1.

The method of data reduction was chosen due to the random nature of tail buffet pressures. As the unsteady buffet pressures measured are assumed to be zero-mean and stationary random process, it was subjected to standard analysis techniques in the time and frequency domains. The surface pressure fluctuations were used to calculate root-mean-square (RMS) values and power spectral densities (PSD) of the buffet pressures. Differential pressure time histories were computed at each transducer-pair station for each test condition by subtracting the outer surface pressure reading from the inner surface pressure reading at each time step. Root-mean-square values and power spectral densities of differential pressure time histories were then obtained as follows.

3.1 Root Mean Square Values of Buffet Pressure

The time-averaged fluctuating component $P'(\mathbf{r})$ of unsteady pressure $P(\mathbf{r},t)$ on the tail surface was found as the root-mean-square value of instantaneous buffet pressure

$$P'^2(\mathbf{r}) = \frac{1}{t}\int (P(\mathbf{r},t) - \overline{P}(\mathbf{r}))^2 \; dt, \tag{1}$$

where $\mathbf{r}$ is a coordinate vector of a pressure transducer,
$\overline{P}$ is the mean static pressure,
t is time.

Note, that all the dynamic data provided to AMRL contained only the fluctuating component of buffet pressures. Thus, the mean static pressure computed from the digitised signals was essentially zero for all the transducer locations.

The zero-mean RMS differential buffet pressure $\Delta P'(\mathbf{r})$ for each pair of pressure transducers at the vertical tail provides a measure of the average fluctuations of unsteady net pressure and was determined as

$$\Delta P'^2(\mathbf{r}) = \frac{1}{t}\int (P_{in}(\mathbf{r},t) - P_{out}(\mathbf{r},t))^2 \; dt, \tag{2}$$

where P_{in} is inner surface unsteady pressure,
P_{out} is outer surface unsteady pressure.

It has been shown by Mabey [1] that unsteady buffet pressures can be effectively normalised with the free-stream dynamic pressure q_∞, allowing the elimination of the free-stream velocity U_∞ from the list of parameters. Thus, the RMS differential pressure coefficient for each of the transducer pairs was defined as

$$C'_{\Delta P}(\mathbf{r}) = \Delta P'(\mathbf{r}) / q_\infty, \tag{3}$$

where $q_\infty = \rho_\infty U_\infty / 2$ and ρ_∞ is free-stream air density. Using the differential pressure in non-dimensional form allows analysis and comparison of buffet pressure characteristics measured in sub-scale and full-scale experiments.

3.2 Power Spectral Density of Buffet Pressure

Another important characteristic in buffet studies is the power spectral density of the unsteady component of the differential pressure coefficient denoted as $C''_{\Delta P}$. The differential pressure time histories from each test condition were converted into the frequency domain using single-sided periodogram utilising Fast Fourier Transform (FFT) technique, which is a classical method of PSD estimation.

The wing's mean aerodynamic chord was chosen as the characteristic length $\bar{c}$ for processing the unsteady pressure results in order to provide consistency with that used in previous buffet research, such as Zimmennan and Ferman [12].

To determine a time-averaged PSD function, the 32-second time record, which contained 16194 valid data points, was subdivided into records which contained 1024 samples and were overlapped by 50%. A Hanning window was applied to each record to reduce bandwidth leakage. PSDs were calculated for each record and averaged to yield a time-averaged PSD to increase statistical confidence. The variation of the PSDs with time for any signal was found to be quite significant and time averaging was required to reduce error in the PSD estimates.

The non-dimensional form of the buffet pressure PSD was suggested by Mabey [1] and may be expressed in terms of the free-stream dynamic pressure as

$$\left(\frac{P'(\mathbf{r})}{q_\infty}\right)^2 = \int_{n=0}^{n=\infty} F(n)dn = \int_{\ln n=-\infty}^{\ln n=+\infty} nF(n)d(\ln n). \tag{4}$$

Here $F(n)$ is the non-dimensional power spectral density of buffet pressure fluctuations and is essentially a PSD of unsteady pressure coefficient $C_{\Delta P}(\mathbf{r})$ divided by the characteristic time scale $\bar{c}/U_\infty$.

The reduced frequency n may be expressed as the Strouhal number of differential pressure fluctuations

$$n = \frac{f\bar{c}}{U_\infty}, \tag{5}$$

where f is frequency of pressure fluctuations.

Following recommendations from Mabey, the computed buffet pressure spectra plots were analysed and presented as $\sqrt{nF(n)}$ versus reduced frequency n.

4. Modelling of Vertical Tail Buffet

It is known that buffet data are extremely difficult to model using traditional regression techniques due to the multiple number of noisy parameters that interact in a non-linear manner, see Ferman *et al.* [13]. So it was suggested that Artificial Neural Networks (ANN) are especially adept at modelling this kind of data because their inter-connected algorithms can accommodate these nonlinearities, see Jacobs *et al.* [14]. One of the major features of neural networks is their ability to generalise, that is, to successfully classify patterns that have not been previously presented, which makes them a good candidate for sparse data modelling.

4.1 Artificial Neural Network Architectures

Artificial neural networks can be characterised as 'computational models' with particular properties such as the ability to adapt or learn, to generalise, and to organise data. The ANNs are described as massively connected networks whose operation is based on parallel processing. However, many of the above-mentioned properties can be attributed to existing non-neural models and the question exists whether the neural approach is better suited for a particular applications than conventional models.

Neural networks appear unique in their ability to extract the essential features from a training set and use them to identify new inputs. Neural networks generalise by detecting features of the input pattern that have been learnt to be significant, and so coded into the internal units. Thus an unknown pattern is classified with others that share the same distinguishing features. This means that learning by example is a feasible approach, since only a representative set of patterns has to be taught to the network, and the generalisation properties will allow similar inputs to be classified as well. It also means that noisy inputs will be classified, by means of their similarity with the pure input. It is this generalisation ability that allows artificial neural networks to perform more successfully on real-world problems than other pattern recognition or expert system methods, see Krose & van der Smagt [15].

In general, neural networks are good at interpolation, but not so good at extrapolation. They are able to detect the patterns that exist in the inputs they are given, and allow for intermediate states that have not been seen. However, inputs that are extensions of the range of patterns are less well classified, since there is little with which to compare them. Thus, given an unseen pattern that is an intermediate mixture of two previously taught patterns, the net will classify it as an example of the predominant pattern. If the pattern does not correspond to anything the net has seen before, then prediction will be much poorer.

4.1.1 Multi-Layer Perceptron

Multi-layered feed-forward networks are arguably the most popular neural network architecture, and certainly the trigger of the widespread explosion of activity in this area. This type of neural network usually has multiple processing units or nodes, with weights and biases as adjustable parameters. The network is arranged in several layers where nodes in adjacent layers are interconnected. If smoothly limiting non-linear sigmoid (S-shaped) transfer function

$$\phi(t) = \frac{1}{1+e^{-t}}, \tag{6}$$

or hyperbolic tangent are used in a multi-layer feed-forward network then this network architecture is often called the Multi-Layer Perceptron (MLP).

This MLP network architecture is also known by the name of the algorithm used to train it, back error propagation (BP), see Rumelhart *et al.* [16]. Comparison with the desired response enables the weights to be altered so that the network can produce a more accurate output next time. This is achieved by adjusting the weights on the links between the units, and the training algorithm does this by calculating the value of the error function for that particular input, and then back-propagating the error from one layer to the previous one. Each unit in the net has its weights adjusted so that it reduces the value of the error function.

The learning algorithm for MLP networks usually performs some variants of gradient descent, altering the value of each weight or bias parameter in the direction for which the change in that particular parameter moves the output activity patterns nearer to their target values. This training method can also trap the network configuration in local minima of the error function that stops the training process.

Another problem inherent in feed-forward networks is overfitting, when after successful training on a large dataset the network fails to generalise to new inputs. Here, the size of the network has to be chosen such that it is just powerful enough to provide an adequate fit. However, finding an optimal size of the network to prevent overfitting is a difficult task and requires extensive testing. One of the methods for improving network generalisation is to use an optimal regularisation technique such as Bayesian regularisation, see MacKay [17]. It is recognised that more complex models can always fit the data better, so the most likely model choice would lead to an implausible over-parameterised model that will generalise poorly. Bayesian methods embody the principle of Occam's razor [17] that states that unnecessarily complex models should not be preferred to simpler ones and complex models are automatically self-penalised under Bayes' rule. Bayesian regularisation provides a measure of how many network parameters are being effectively used by the network and sets the optimal performance function to achieve the best generalisation.

Although the MLP network can have an arbitrary number of layers, it is stated by the universal approximation theorem, that only one layer of hidden units suffices to approximate any function with finitely many discontinuities to arbitrary precision, provided the transfer functions of the hidden units are non-linear, see [18, 19].

4.1.2 Radial Basis Functions

An enhancement to the standard multilayer perceptron techniques uses what is called the radial basis functions. These are a set of generally non-linear functions that are built up into one function that can partition the pattern space. The usual multilayer perceptron builds its classifications from hyperplanes, whereas the radial basis approach uses hyperellipsoids to partition the pattern space.

A radial basis function (RBF) network used to approximate an unknown function f can be described by affine mapping

$$f(\mathbf{x}) \approx w_0 + \sum_{i=1}^{m} w_i \phi_i(\mathbf{x}), \tag{7}$$

in which the m radially-symmetric basis functions ϕ_i are often taken to be translated dilations of a prototype RBF

$$\phi_i(\mathbf{x}) = \phi(\|\mathbf{x} - \mathbf{c}_i\| / d_i), \tag{8}$$

where c_i is the centre of basis function,

d_i is a scaling factor or width for the radius $\|\mathbf{x} - \mathbf{c}_i\|$,

w_i is an adjustable parameter or weight.

Choices of ϕ considered in theoretical investigations and practical applications include linear $\phi(r) = r$, cubic $\phi(r) = r^3$, thin plate spline $\phi(r) = r^2 \log r$, multiquadric $\phi(r) = \sqrt{r^2 + 1}$ or Gaussian $\phi(r) = e^{-r^2/2}$ functions, see [19,20].

The central problem in finding the solution is the placement of the centres $\mathbf{c}_i$ and determination of the radial scaling factors d_i to achieve the best prediction and generalisation performance, see Chen *et al.* [20]. This problem is most often approached by clustering the input data points so that the centres of these clusters are then used as the RBF centres $\mathbf{c}_i$. Clustering is typically performed by a vector quantisation algorithm, which iteratively minimises some measure of distortion such as the mean-squared from each data point to the centre of the cluster to which it belongs.

Once the centres and widths of the basis functions are determined, each weight w_i used in the approximation of (7) may be determined either by direct numerical least-squares methods such as singular value decomposition or by iterative methods such as an orthogonal least squares learning algorithm. Since these coefficients are added in a linear fashion, the problem is an exact one and has a guaranteed solution since there are no nasty local minima situations in which to fall.

This approach is guaranteed to produce a function that fits all the data points, as long as there is a basis function for each input to be classified. Having one basis function for each input does mean that noisy or anomalous data points will also be classified, however, and these will tend to cause distortion. This noise distortion causes problems with generalisation and since the classification surface is not necessarily smooth, very similar inputs may find themselves assigned to very different classes. The solution to this is to reduce the number of basis functions to a level at which an acceptable fit to the data is still achieved.

The use of radial basis functions is attractive, since they need only linear optimisation techniques, which provide a guaranteed, globally optimal solution. The difficulty in using them is in deciding on the set of transfer functions to be used, in order to get an adequate fit to the data.

4.2 Modelling the RMS Values of Buffet Pressures

Buffet data provided from the full-scale F/A-18 tail buffet test contained the inboard and outboard pressure histories as a function of free stream dynamic pressure, angle of attack, angle of sideslip and position of the pressure sensors. Since dynamic excitation of the vertical tail depends on the net contribution of unsteady loads, the buffet loading was described in terms of differential buffet pressures measured at each of the transducer pairs. As the unsteady buffet pressures can be normalised with the free-stream dynamic pressure, the buffet loads were reduced to differential pressure coefficients that allow for easy incorporation of other experimental and flight data into the integrated buffet database.

Only one aircraft configuration with LEX fence off was selected for the analysis. All available test conditions in this configuration were examined and 73 representative test points with unique combinations of angles of attack and sideslip were selected to form a training set, see Figure 4. The set of network input parameters included angle of attack, angle of sideslip, chordwise and spanwise locations of pressure transducer with RMS value of differential pressure as the network output. A total of 1168 input/output pairs was available for neural network training and validation. Note, that one particular test point supposedly acquired at 50 degrees angle of attack and -10 degrees of angle of sideslip was not included in the training set as its test conditions were not positively identified. This test point was used later for validation of network generalisation abilities.

Two neural network architectures were initially investigated in order to assess their ability to model the buffet data, namely the Multi-Layer Perceptron (MLP) network trained with Back Propagation (BP) and the Radial Basis Function (RBF) network trained with an orthogonal least squares algorithm. For the case of the RBF network, an appropriate set of transfer functions to be used for buffet data modelling was determined on a sample buffet data. Several transfer functions including Gaussian, cubic, multiquadric and inverse multiquadric functions were assessed for function approximation, interpolation and extrapolation tasks. It was found that for most of the transfer functions evaluated, the outputs unrealistically diverged or approached zero, as testing inputs were placed further away from the nearest training input. Transfer functions with such a property cannot be used for extrapolation or even interpolation over long distances.

After extensive experimentation it was concluded that an RBF network with multiquadric transfer functions is better suited for buffet modelling as it provides acceptable fit to complex functions and allows for function extrapolation. This is consistent with the findings of Jacobs *et al.* [14], who also employed multiquadric transfer functions for sparse buffet data modelling. An example of RBF network evaluation with different transfer functions for approximation and extrapolation tasks is presented in Figure 5 where two last data points were excluded from the training set. As one can see, the RBF network with multiquadric functions performed well for both the function approximation and extrapolation while conventional Gaussian transfer functions showed unsatisfactory results in both tasks.

Initially, the ability of the ANN to predict the RMS differential pressures along the vertical tail at various test conditions was investigated on two reduced datasets where one set contained only data acquired at various angles of attack and zero sideslip and the other included data measured at 30 degrees angle of attack and variable sideslip. The datasets were broken down by angle of attack into a training set and a test set to show generalisation of the neural network to new inputs. The output RMS pressures were generated at a fine grid of evenly spaced points along the surface of the tail and then interpolated using tension splines.

It was concluded that both the MPL and RBF networks performed reasonably well in estimating the pressure distribution along the tail, see Figure 6 - Figure 13. As there was no restriction placed on the complexity of the networks, the RBF network was able to fit all the data points with a specified accuracy. Thus, no test pressure distributions are presented here for comparison as the results generated by RBF network closely match the test data and can be used as a reference.

Comparison of pressure maps generated by MPL and RBF network architectures shows that the results are quite similar for most of the test conditions. However, some inconsistency in magnitude of RMS differential pressures can be observed for moderate negative values of sideslip, where pressure distribution produced by the RBF network

appeared to better match the training data, see Figure 10. It was found that the use of supervised training is required to improve accuracy of MLP network predictions. Despite this shortfall, the MLP network still appeared to be more suitable choice for modelling the buffet data since it had the best training time and greater generalisation capability by capturing the most significant features in the training dataset.

After showing that both of the neural networks can generalise well after training on the reduced datasets, the next step was to find if reasonable pressure distribution can be predicted at any angles of attack and sideslip over the entire test matrix. In this case, both the networks were presented with all the available data and allowed to train until the convergence of performance functions. Although the MLP showed the most promise for buffet modelling during initial trials, the network training on a complete set of data encountered serious difficulties. Numerous attempts to train MLP network failed to produce a satisfactory solution, as the trained network showed an unacceptable fit to existing data and poor generalisation.

The use of Bayesian regularisation to optimise network parameters did not improve the training results as, in most of the cases, the search vector tended to settle at the local minimum preventing further training progress. After exhaustive testing of various algorithms for feed-forward network training [21, 22] it was concluded that existing learning methods cannot accommodate complex non-linear relations in buffet data. Here, the use of global optimisation techniques such as evolutionary and genetic algorithms combined with Bayesian regularisation may be required to determine an optimal set of network parameters. This is left for future studies.

The difficulties experienced with the MLP network training prevented its further use in the study and only an RBF network with multiquadric functions was used in following investigations.

Having established the ability of the RBF network to interpolate over the tail surface, pressure maps were generated for test conditions of 50 degrees angle of attack and –10 degrees of sideslip, as this test point was originally excluded from the training set, see Figure 14. Comparison of computed and measured results revealed remarkable similarity of patterns and RMS values of differential pressure distribution allowing the identification of the test conditions of the suspected test point and confirming the prediction abilities of the network.

To ensure that RBF network could accomplish distance interpolation, the data measured from the pressure transducer pair at 60% span, 45% chord location on the tail were removed from the training set. The trained network was then tested to verify its ability to predict the pressures near the centre of the tail for various angles of attack and sideslip.

It was found that the RBF network is able to predict the missing data reasonably well. As one can see from the error map in Figure 15, for most of the test conditions, the

network's predictions were fairly accurate with maximum error well below 15%. Only in limited regions of high angle of attack and negative sideslip did the prediction error reached 35% possibly due to the presence of large local pressure gradients, which affected the network prediction ability, especially if training occurred on a coarse grid of pressure sensors.

4.3 Modelling the Spectral Content of Buffet Pressures

The next step was to assess the network's ability to predict the Power Spectral Density (PSD) of differential buffet pressures on the tail. Again, the test point at 50 degrees angle of attack and -10 degrees of sideslip was selected for validation. The training set contained spectral characteristics of buffet pressure data for all the other angles of attack and sideslip in the form of PSD functions, each containing the 513 nondimensional frequencies and their corresponding outputs (nondimensional pressure spectra values). The network was expected to predict power spectral densities of buffet pressures at any point over the tail surface at new input conditions.

It should be noted that the average magnitude of the buffet pressure spectrum values can vary significantly over the frequency range, as buffet energy is concentrated in a relatively narrow frequency band. Because of the variation of dominant frequencies with test conditions and large scatter of pressure power values, it was found impractical to characterise the spectral content of buffet pressures in terms of the shape of PSD curve alone. In order to equally emphasise both the lower and higher spectral density magnitudes, a PSD prediction system has been developed by utilising an independent RBF network for each of the spectral lines and combining output from all of the basic networks to predict the complete PSD curve. Thus, it is assumed that the magnitude of power spectral density at a particular spectral line is independent of the rest of the spectrum. The choice of RBF architecture for each of the basic networks was based on its robustness and greater interpolation ability.

The network system was developed as having four inputs (angles of attack and sideslip and coordinates of each pressure transducer) and 513 outputs (pressure spectrum magnitudes) at corresponding nondimensional frequencies. A total of 599,184 input/output pairs formed a training set. The spectral content of the buffet pressure was predicted over the tail surface and comparison of predicted and measured PSD curves for selected locations are presented in Figure 16 - Figure 18. Note that, for clarity, only the most significant part of the spectrum is presented on the plots.

As shown by the results, the neural network system is able to predict the correct shape of the PSD curves as well as to identify dominant frequencies in the PSD spectra. It is also able to follow sharp changes in the PSD curve, as may be noticed in Figure 18, where differential pressure data at 30% span, 90% chord location were found to be contaminated by a narrow-band extraneous signal.

Despite some discrepancy in the prediction of power pressure values, the network's ability to reproduce the overall trends of the PSD curves confirmed the validity of the adopted approach. It is anticipated that the neural network system can also be used to model other important buffet characteristics such as spatial correlation and frequency response functions between unsteady pressures on the tail, which are required for correct simulation of buffet loading.

Most of the experimental buffet data obtained so far [5, 6] are measured on a finite grid of pressure transducers limiting our knowledge of dynamic pressure distribution on the rest of the tail. Numerical simulations of vertical tail buffet loading can provide some insight into pressure distributions in the areas where the buffet data have not yet been acquired, see Levinski [11]. The results of numerical simulations can be used to supplement the sparse experimental data allowing the ANN buffet prediction system to generate pressure maps over the entire tail surface.

5. Conclusions

The feasibility of using artificial neural networks for predicting empennage buffet pressures as a function of geometric conditions has been investigated. The buffet loads prediction method is developed which depends on experimental data to train the ANN algorithm and which is able to expand its knowledge base with additional data. Aerodynamic pressures obtained from a full-scale F/A-18 tail buffet test in the 80ft X 120ft test section of NASA Ames National Full-Scale Aerodynamics Complex (NFAC) provided test bed for the development and assessment of the ANN buffet prediction method.

Two network architectures have been assessed for buffet data modelling. The RBF network with multiquadric functions was selected based on its robustness and good generalisation abilities for differing input conditions. Although the MLP network showed the most promise during initial trials, its training on a large dataset resulted in an unacceptable fit to existing data and poor generalisation. The use of global optimisation techniques such as evolutionary and genetic algorithms combined with Bayesian regularisation should be investigated to determine an optimal set of network parameters during training. Development of a globally optimised training algorithm for MLP networks is left for future study.

The study revealed that artificial neural networks have a great potential as a method for modelling the complex nonlinear relationships inherent in buffet data. The ability of neural networks to accurately predict RMS values and frequency content of unsteady buffet pressures was confirmed. Based on the ANN methodology investigated, a buffet prediction system can be developed to provide detailed information about the F/A-18 vertical tail buffet environment through the use of additional experimental and flight test data, as well as results of computational

unsteady aerodynamics. It will allow for better understanding of empennage buffeting problem and can be used in fatigue usage monitoring systems for fleet aircraft.

References

1. Mabey, D. (1987) Some Aspects of Aircraft Dynamic Loads Due to Flow Separation, AGARD-R-750.
2. Lee, B.H., Brown, D. (1990) Wind-Tunnel Studies of F/A-18 Tail Buffet, *J. Aircraft*, Vol. 29, No. 1, 146-152.
3. Thompson, D.H. (1990) *Water tunnel flow visualization of vortex breakdown over the F/A-18*, Aeronautical Research Laboratory, Flight Mechanics Report 179.
4. Martin, C.A., Thompson, D.H. (1991) Scale Model Measurements of Fin Buffet Due to Vortex Bursting on F/A-18, *AGARD Manoeuvring Aerodynamics*, AGARD-CP-497.
5. Meyn, L. A., James, K. D., (1993) Full Scale Wind Tunnel Studies of F/A-18 Tail Buffet, *AIAA Applied Aerodynamics Conference*, AIAA 93-3519, August 9-11, Monterey, CA.
6. Pettit C.L., Brown D.L., and Pendleton E. (1994) Wind Tunnel Tests of Full-Scale F/A-18 Twin Tail Buffet: A Summary of Pressure and Response Measurements, AIAA Paper 94-3476.
7. Lee, B., Brown, D., Zgela, M., and Poirel, D., (1990) Wind Tunnel Investigation and Flight Tests of Tail Buffet on the CF-18 Aircraft, in *Aircraft Dynamic Loads Due to Flow Separation*, AGARD-CP-483, NATO Advisory Group for Aerospace Research and Development, Sorrento, Italy, April 1990.
8. Bean, D. E. and Lee, B., (1994) Correlation of Wind Tunnel and Flight Test Data for F/A-18 Vertical Tail Buffet, AIAA-94-1800-CP, *12th AIAA Applied Aerodynamics Conference*, Colorado Springs, CO, June 20-22.
9. Kandil, O.A., Sheta, E.F., Massey, S.J. (1996) Twin Tail/Delta Wing Configuration Buffet due to Unsteady Vortex Breakdown Flow, AIAA Paper 96-2517-CP.
10. Gee, K., Murman, S. M., and Schiff, L. B., (1996) Computation of F/A-18 Tail Buffet, *Journal of Aircraft*, Vol. 33, No. 6, November-December.
11. Levinski, O. (2001) *Prediction of Buffet Loads on Twin Vertical Tail Using Vortex Method*, Australian Department of Defence, Aeronautical and Maritime Research Laboratory, DSTO-RR-0217.
12. Zimmerman, N. H., and Ferman, M. A., (1987) *Prediction of Tail Buffet Loads for Design Application*, McDonnel Aircraft Company, Report No. NADC-88043-60.
13. Ferman, M. A., Patel, S. R., Zimmerman, N. H., and Gerstenkorn, G., (1990) A Unified Approach to Buffet Response, *70th Meeting of Structures and Materials Panel*, AGARD 17, Sorrento, Italy, April.
14. Jacobs, J. H., Hedgecock, C. E., Lichtenwalner, P. F., and Pado, L. E., (1994) Use of Artificial Neural Networks for Buffet Environments, *Journal of Aircraft*, Vol. 31, No. 4, July-Aug.
15. Krose, B., van der Smagt, P., (1996) *An Introduction to Neural Networks*, The University of Amsterdam, Eighth edition.

16. Rumelhart, D. E., Hilton, G. E., and Williams, R. J., (1986) Learning Representations by Back-propagating Errors, *Nature*, 323, pp. 533-535.
17. MacKay, D. J. C., (1992) Bayesian Interpolation, *Neural Computation*, Vol. 4, No. 3, pp. 415-447.
18. Beale, R., and Jackson, T., (1991) *Neural Computing: An Introduction*, IOP Publishing, Ltd.
19. Lisboa, P. G. J., (1992) *Neural Networks Current Applications*, Chapman & Hall, Liverpool, UK.
20. Chen, S., Cowan, C. F. N., and Grant, P. M., Orthogonal Least Squares Learning Algorithm for Radial Basis Function Networks, (1991) *IEEE Transactions on Neural Networks*, Vol. 2, No. 2, March.
21. Hagan, M. T., Demuth, H., Beale, M., (1996) *Neural Network Design*, PWS Publishing Company.
22. Demuth, H., Beale, M., (2000) *Neural Network Toolbox, For Use with MATLAB*, The Mathworks, Inc.

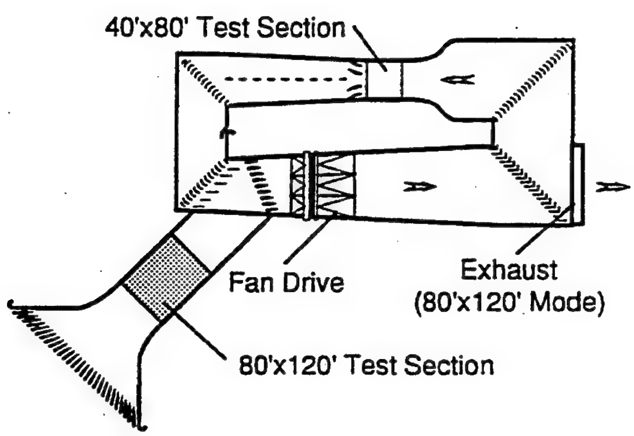

Figure 1 Schematic of National Full-Scale Aerodynamic Complex at NASA Ames Research Centre

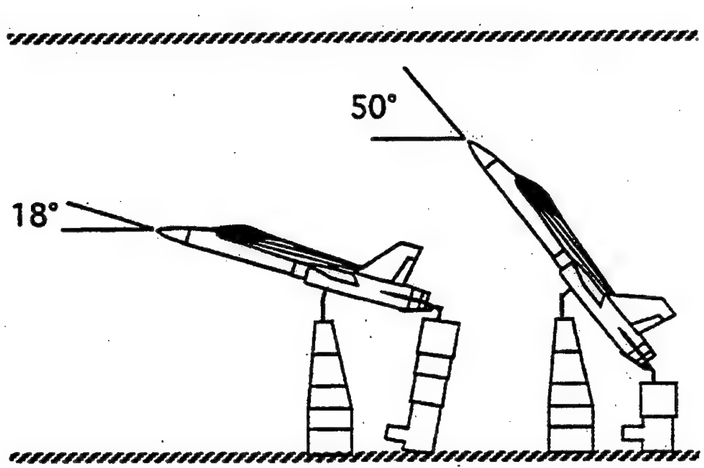

Figure 2 Angle of attack range for test aircraft on struts

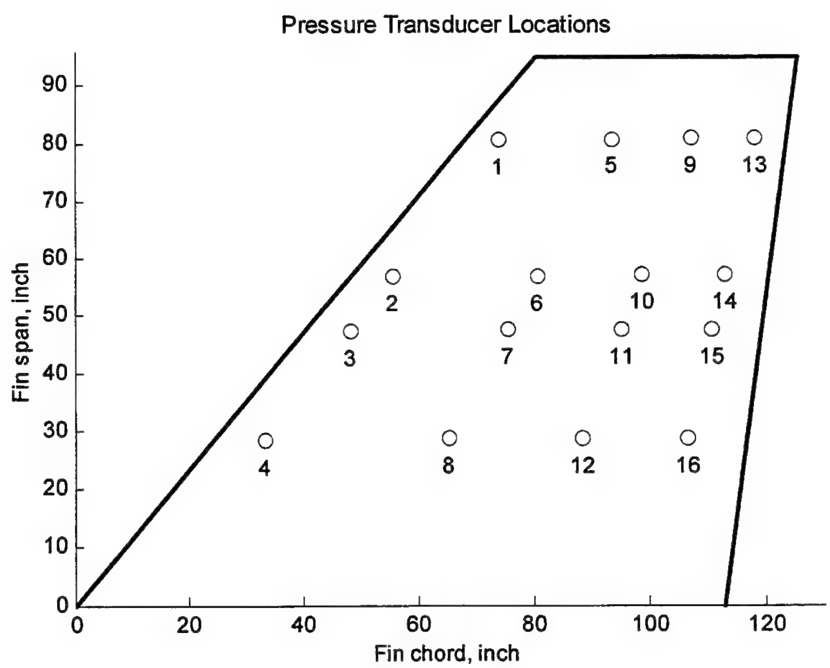

Figure 3 Pressure transducer locations on port vertical tail

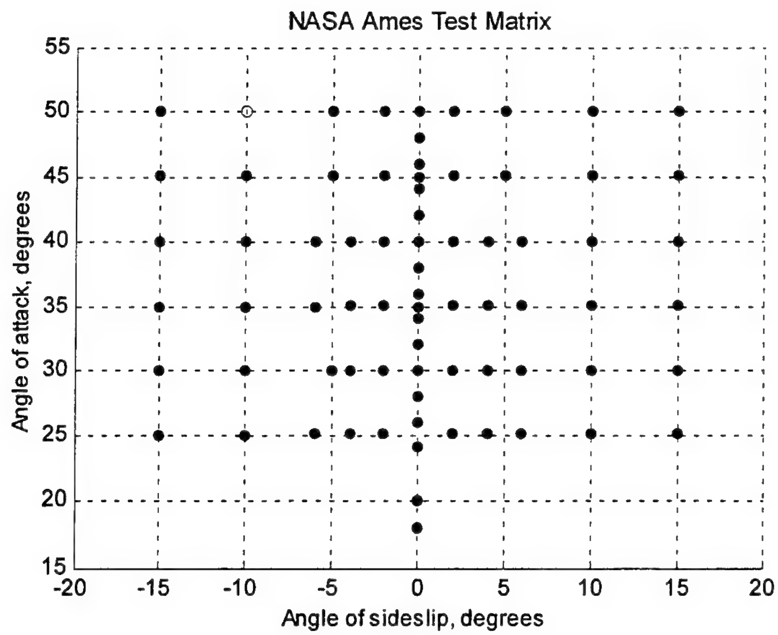

Figure 4 Test matrix for LEX fence off configuration

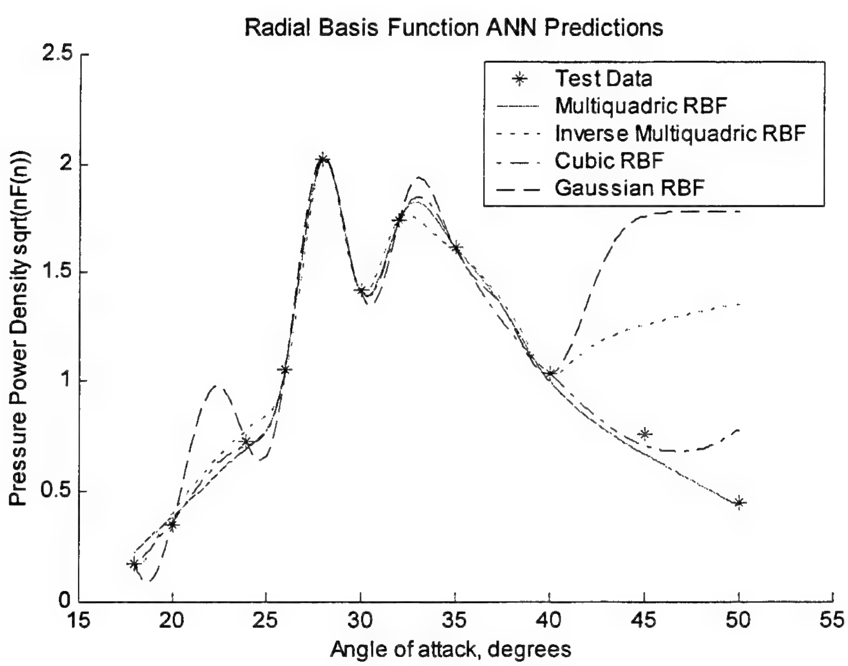

Figure 5 Assessment of RBF network with different transfer functions.

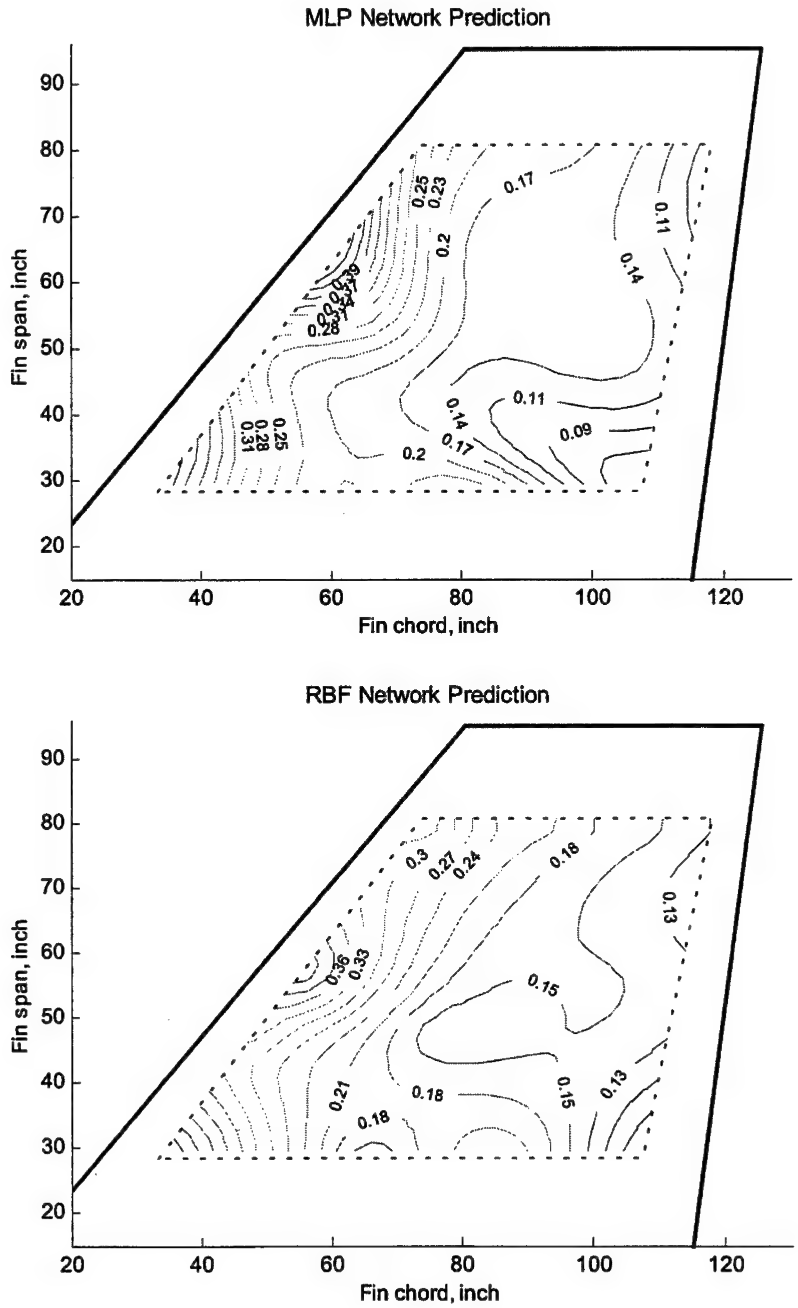

Figure 6 Prediction of RMS differential pressure distribution on vertical tail at 20 degrees angle of attack and zero sideslip

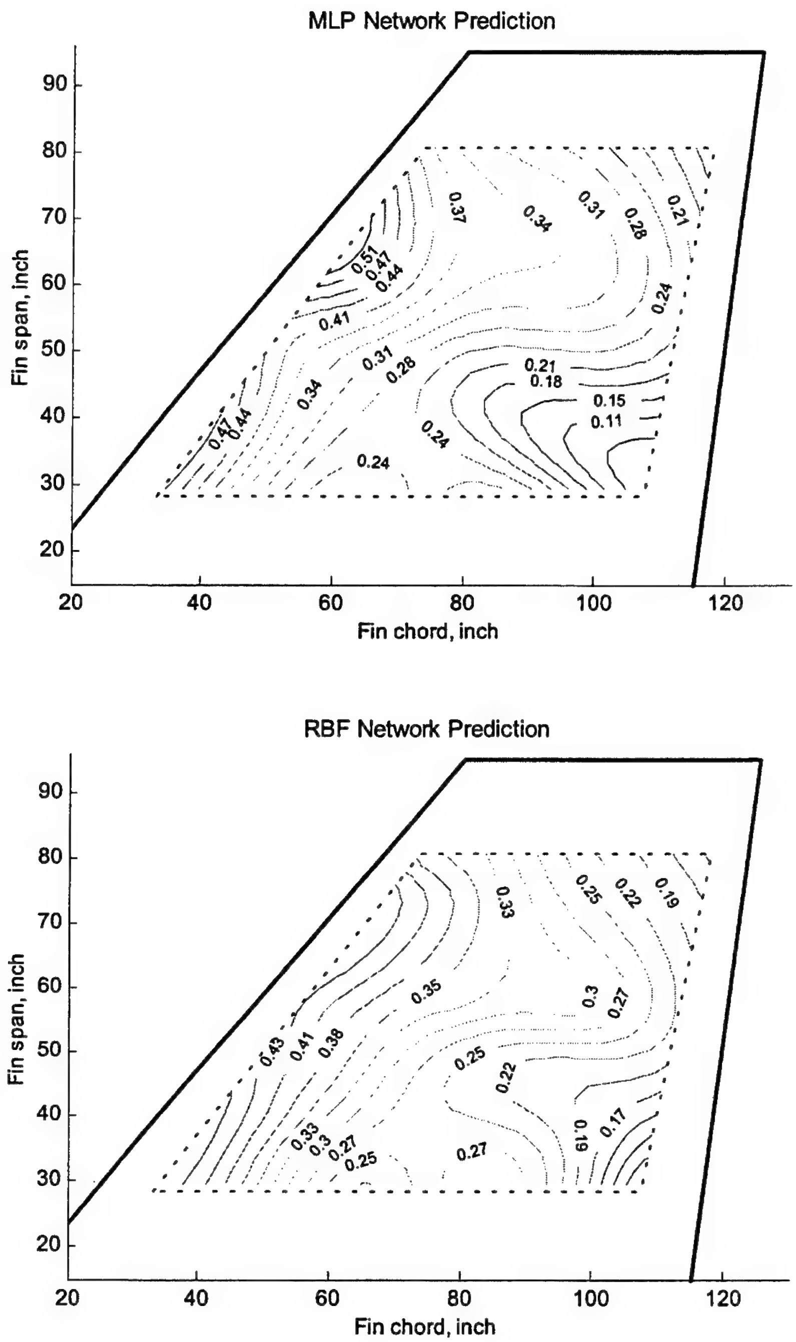

Figure 7 Prediction of RMS differential pressure distribution on vertical tail at 26 degrees angle of attack and zero sideslip

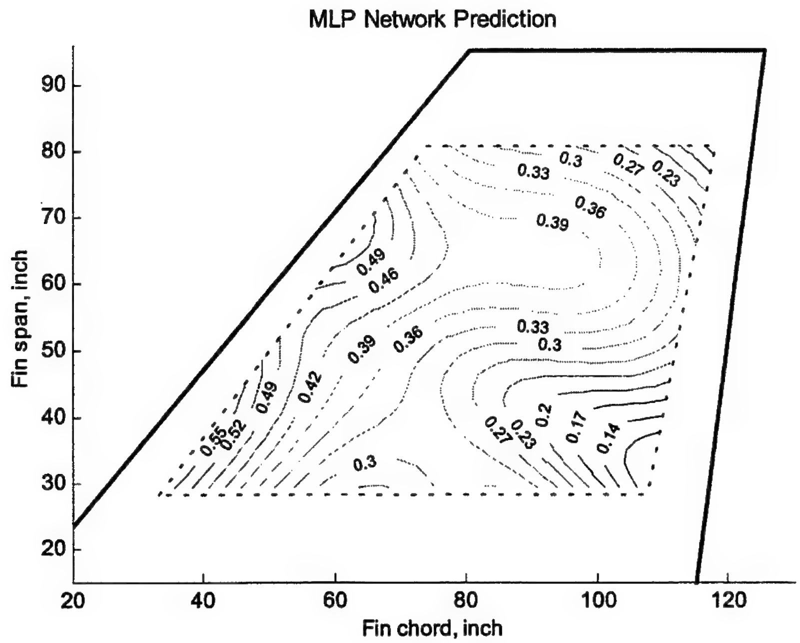

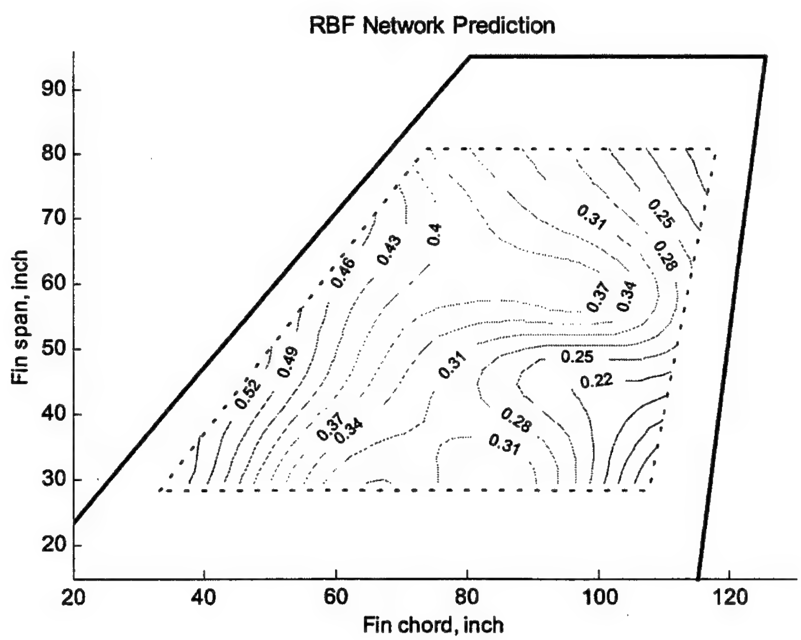

Figure 8 Prediction of RMS differential pressure distribution on vertical tail at 30 degrees angle of attack and zero sideslip

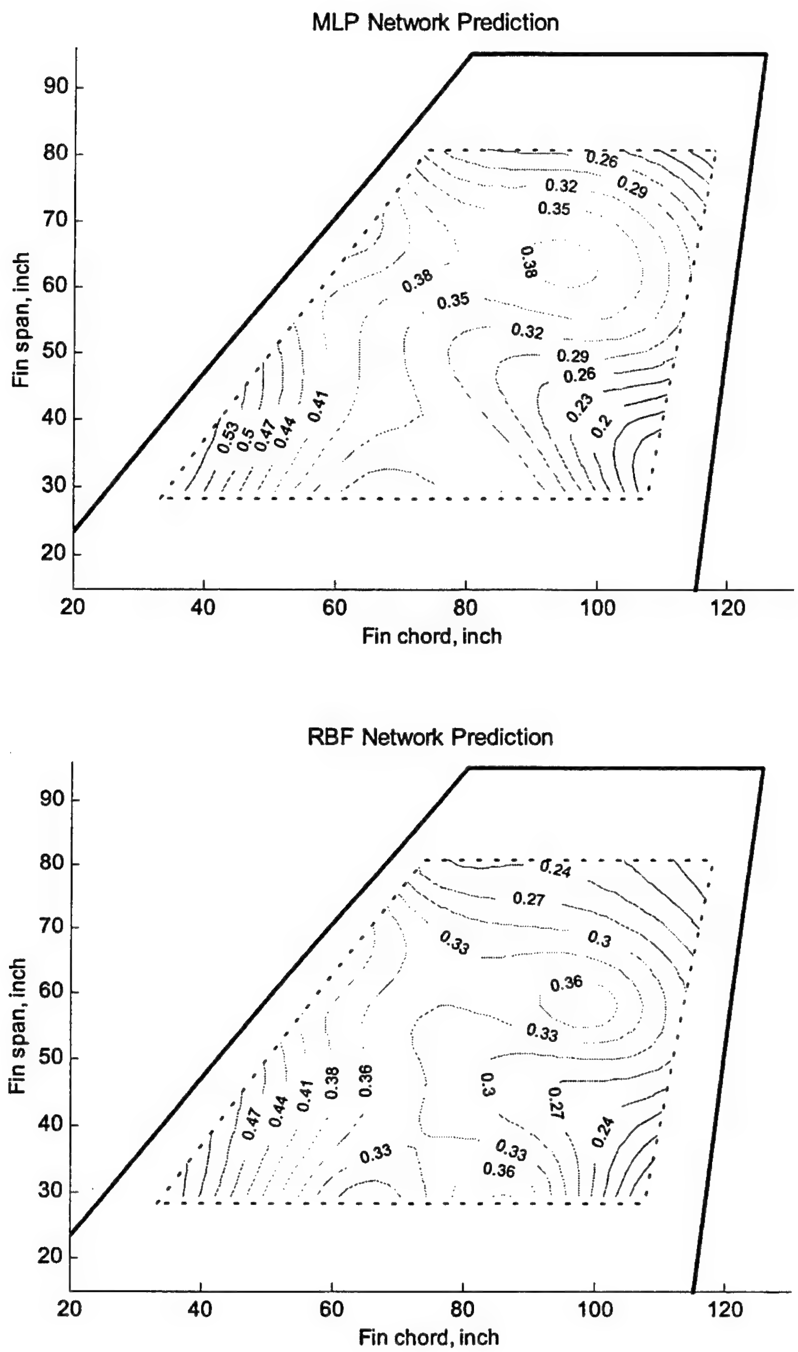

Figure 9 Prediction of RMS differential pressure distribution on vertical tail at 35 degrees angle of attack and zero sideslip

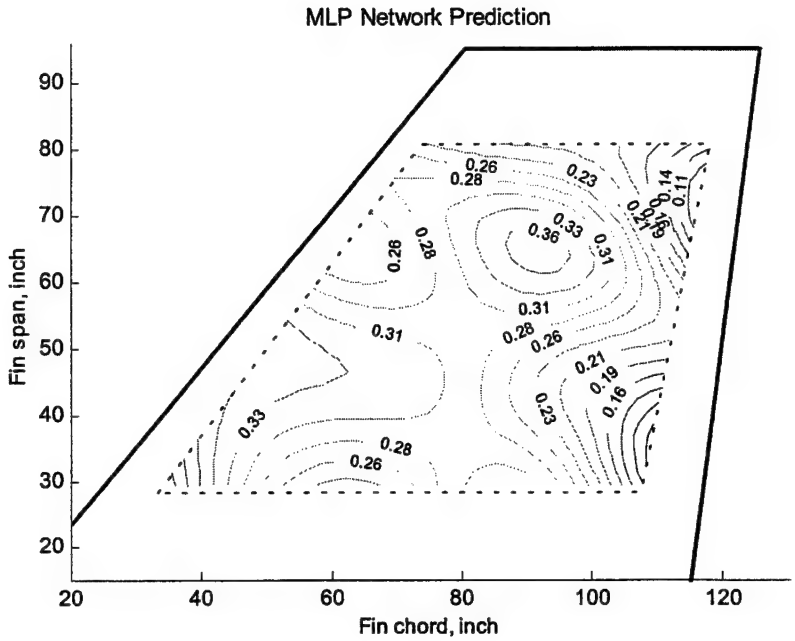

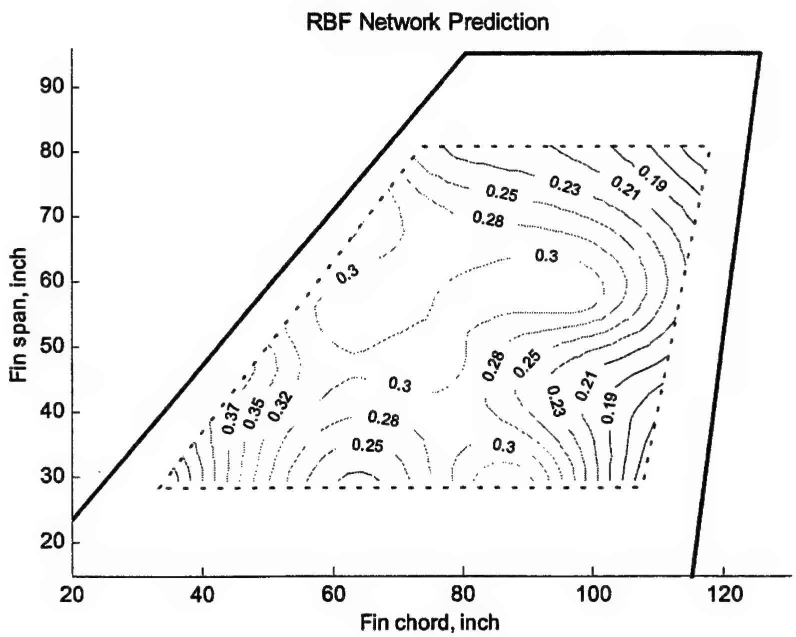

Figure 10 Prediction of RMS differential pressure distribution on vertical tail at 30 degrees angle of attack and 4 degrees angle of sideslip

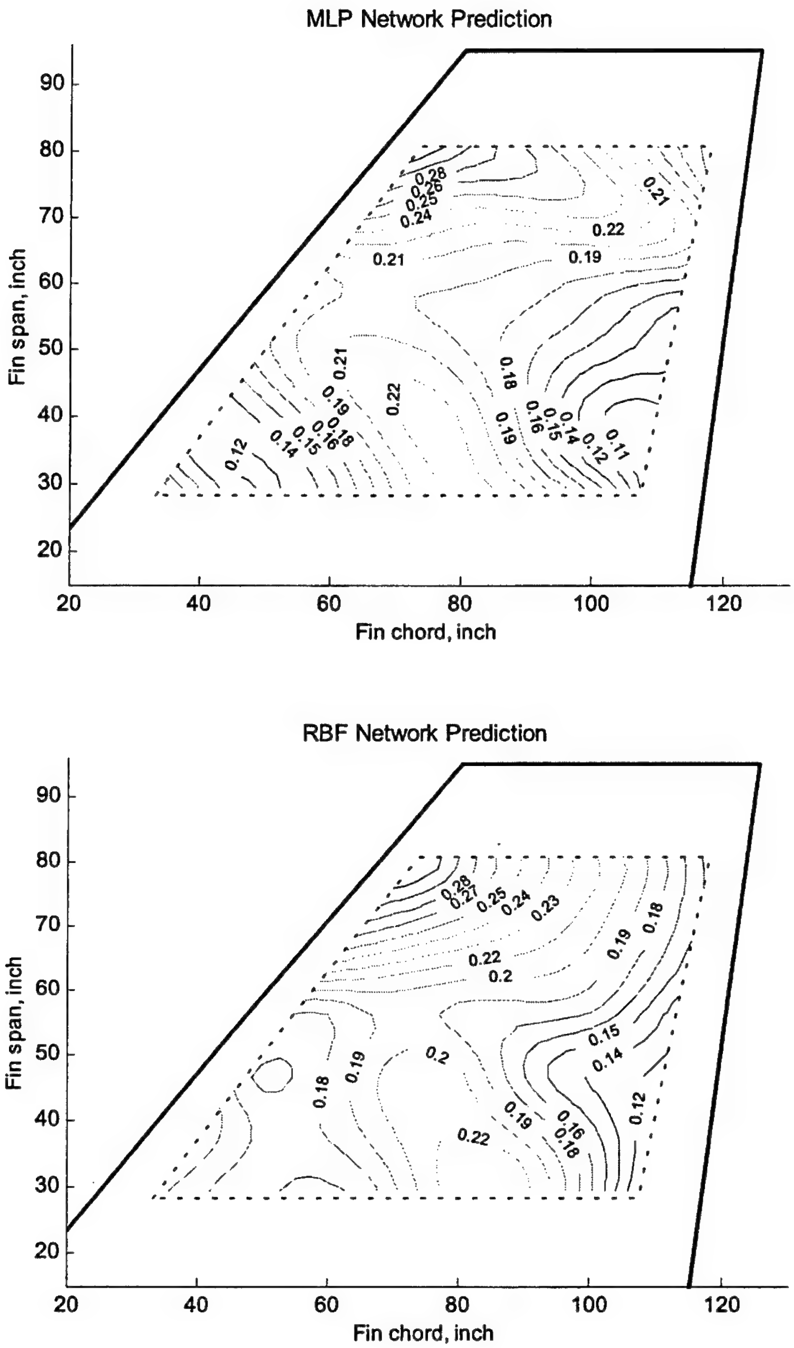

Figure 11 Prediction of RMS differential pressure distribution on vertical tail at 30 degrees angle of attack and 10 degrees angle of sideslip

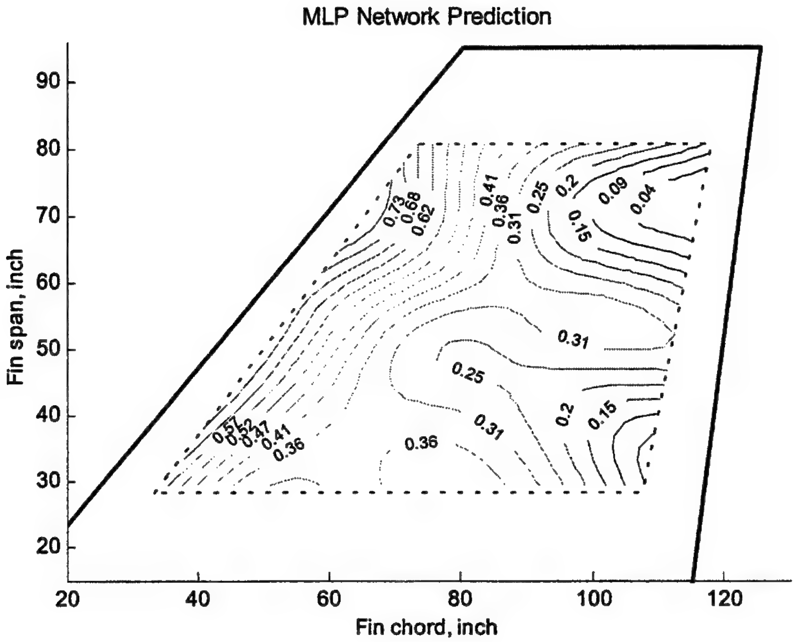

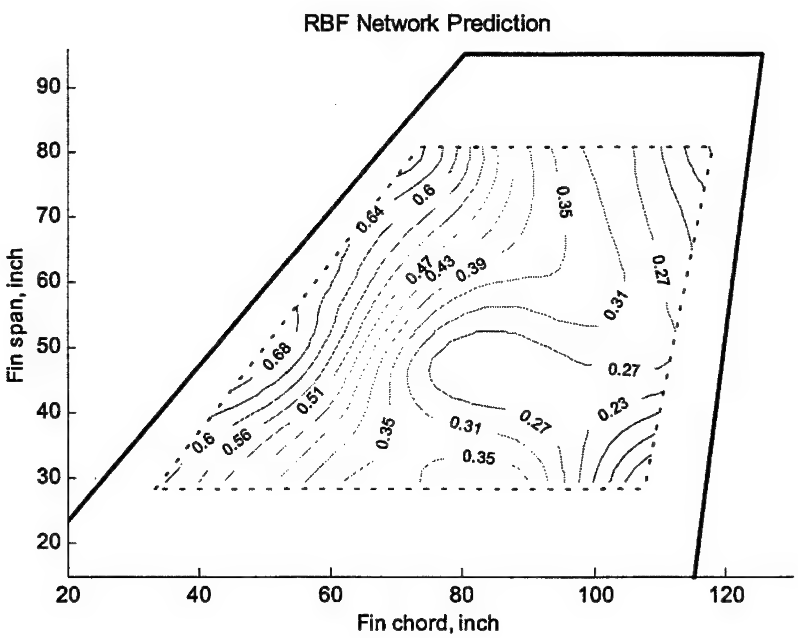

Figure 12 Prediction of RMS differential pressure distribution on vertical tail at 30 degrees angle of attack and -4 degrees angle of sideslip

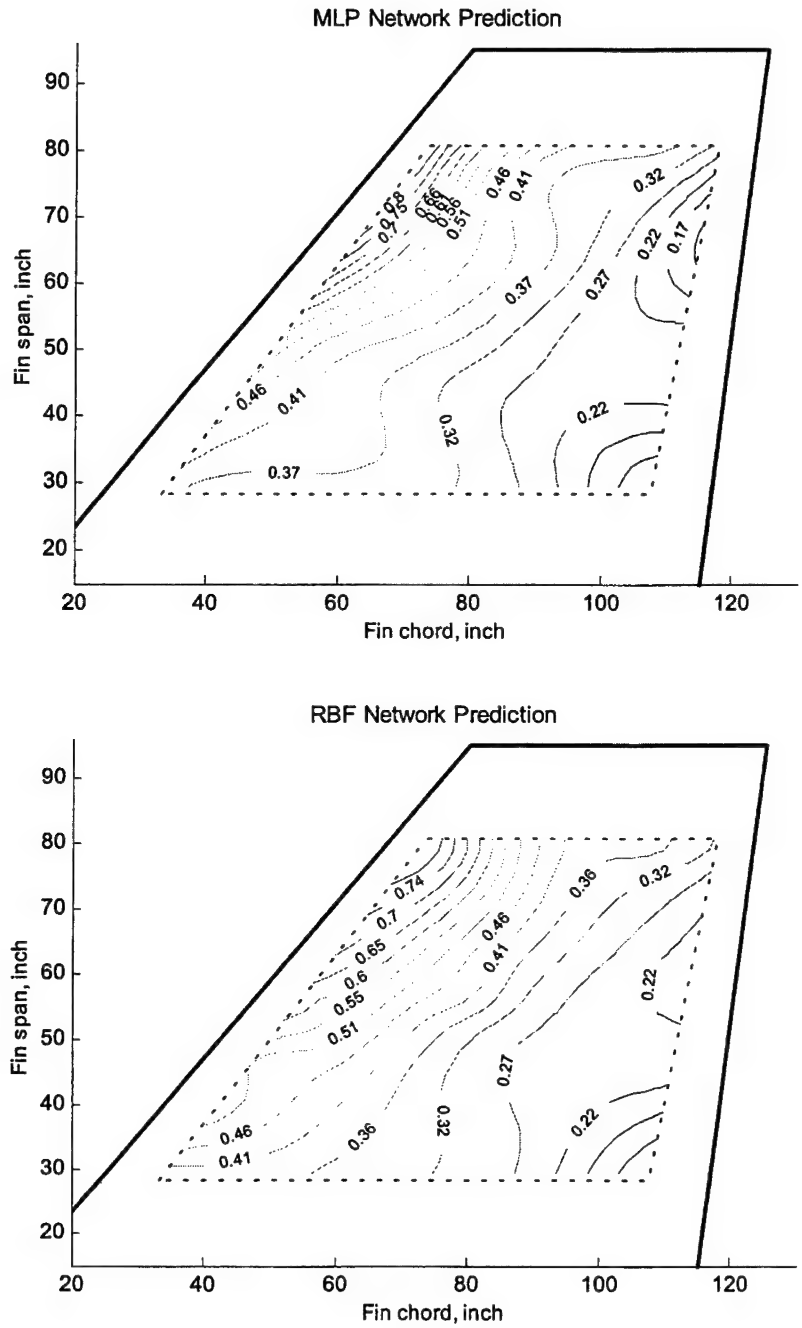

Figure 13 Prediction of RMS differential pressure distribution on vertical tail at 30 degrees angle of attack and -10 degrees angle of sideslip

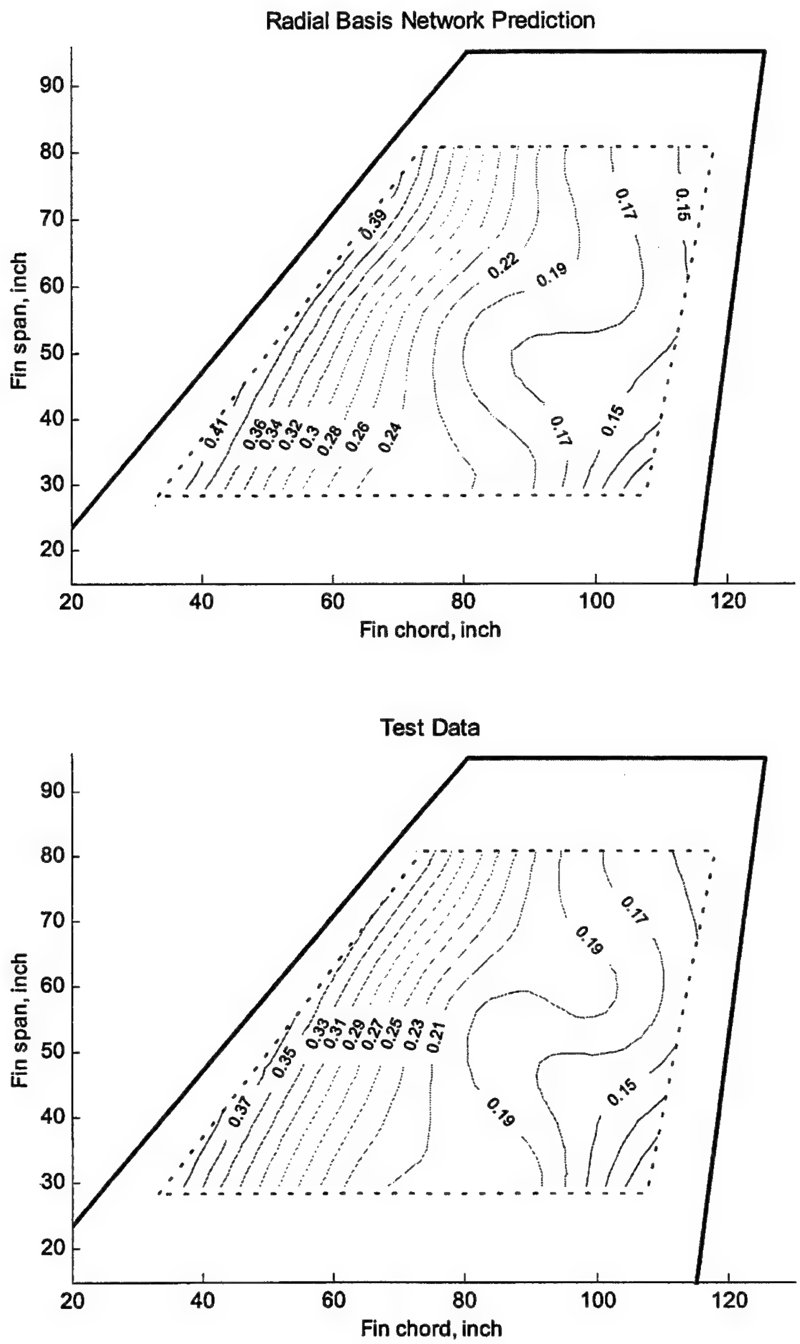

Figure 14 Predicted and measured RMS differential pressure distribution on vertical tail at 50 degrees angle of attack and -10 degrees of sideslip

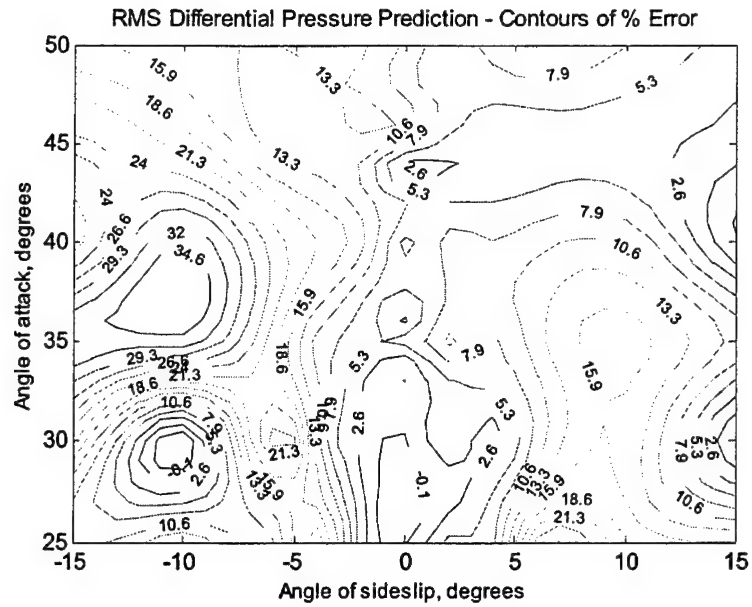

Figure 15 RMS prediction errors at 60% span, 45% chord location on the tail

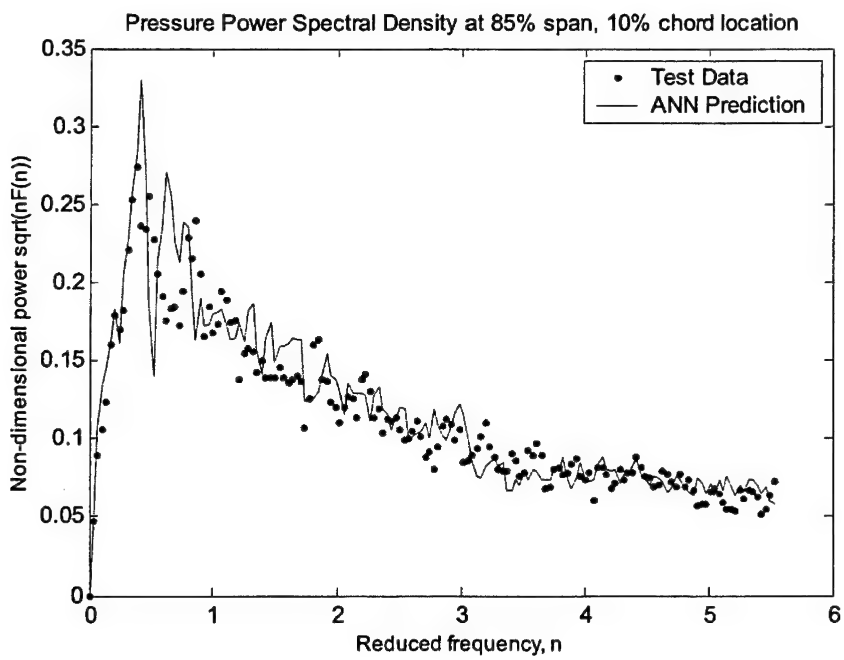

Figure 16 ANN predictions of pressure power density at 50 degrees angle of attack and -10 degrees of sideslip

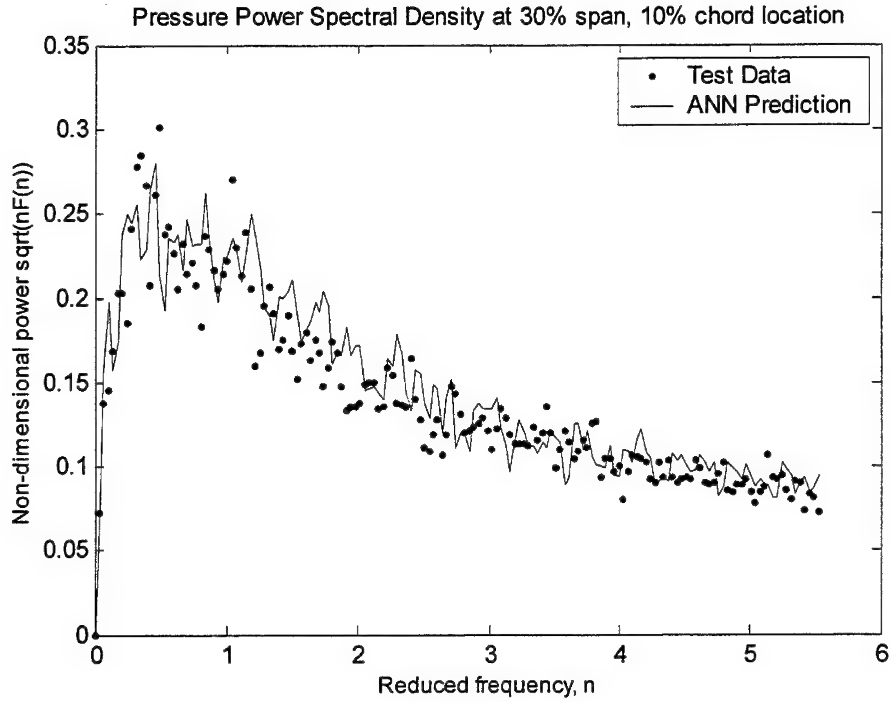

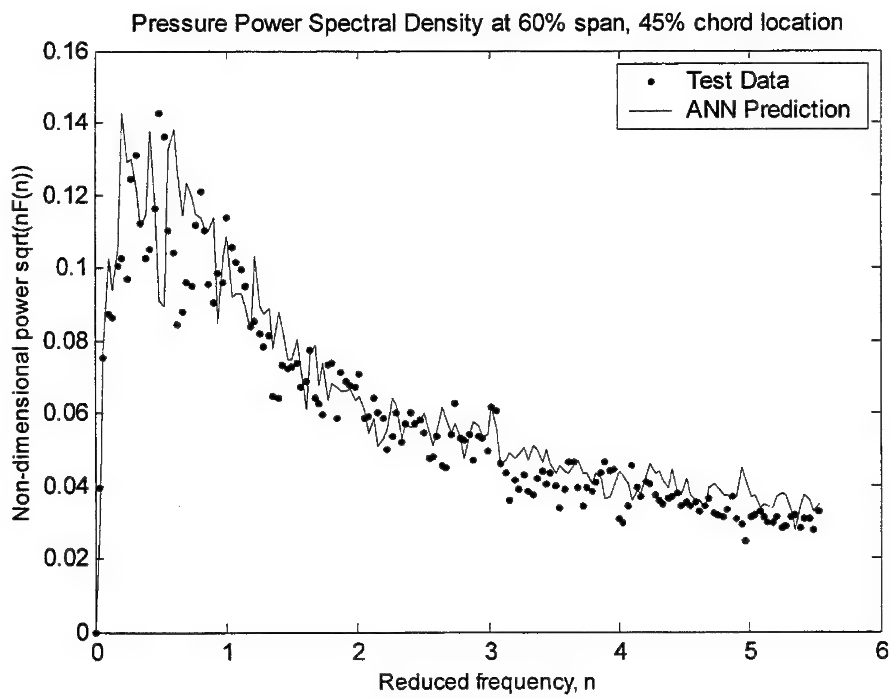

Figure 17 ANN predictions of pressure power density at 50 degrees angle of attack and -10 degrees of sideslip

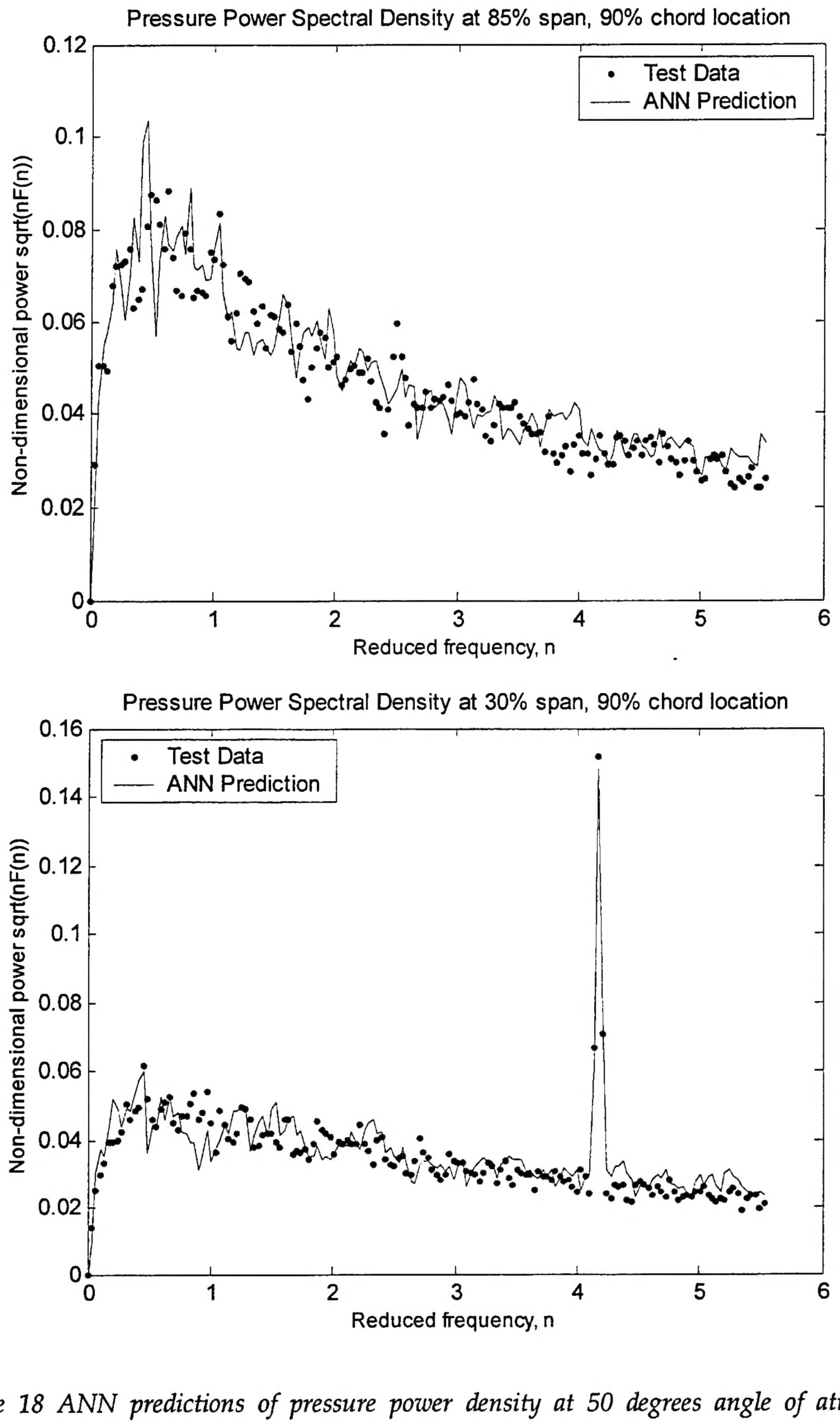

Figure 18 ANN predictions of pressure power density at 50 degrees angle of attack and -10 degrees of sideslip

DISTRIBUTION LIST

Prediction of Vertical Tail Buffet Loads Using Artificial Neural Networks

Oleg Levinski

AUSTRALIA

DEFENCE ORGANISATION

Task Sponsor	**CDR ARDU**	1
S&T Program		
Chief Defence Scientist	shared copy	1
FAS Science Policy		
AS Science Corporate Management		
Director General Science Policy Development		
Counsellor Defence Science, London		(Doc Data Sheet)
Counsellor Defence Science, Washington		(Doc Data Sheet)
Scientific Adviser to MRDC Thailand		(Doc Data Sheet)
Scientific Adviser Joint		1
Navy Scientific Adviser		(Doc Data Sheet and distribution list)
Scientific Adviser - Army		(Doc Data Sheet and distribution list)
Air Force Scientific Adviser		1
Director Trials		1
Aeronautical and Maritime Research Laboratory		
Director		1
Chief of Airframes and Engines Division		1
Research Leader		1
Task Manager (Peter Farrell)		1
Author: Dr. Oleg Levinski		2
Loris Molent		1
David Conser		1
DSTO Library and Archives		
Library Fishermans Bend		(Doc Data sheet)
Library Maribyrnong		(Doc Data sheet)
Library Salisbury		1
Australian Archives		1
Library, MOD, Pyrmont		(Doc Data sheet)
US Defense Technical Information Center		2
UK Defence Research Information Centre		2
Canada Defence Scientific Information Service		1
NZ Defence Information Centre		1
National Library of Australia		1
Capability Development Division		
Director General Maritime Development		(Doc Data Sheet)
Director General Aerospace Development		(Doc Data Sheet)

Knowledge Staff

Director General Command, Control, Communications and Computers (DGC4) (Doc Data Sheet only)

Army

Stuart Schnaars, ABCA Standardisation Officer, Tobruk Barracks, Puckapunyal, 3662 (4 copies)

SO (Science), Deployable Joint Force Headquarters (DJFHQ) (L), MILPO Gallipoli Barracks, Enoggera QLD 4052 (Doc Data Sheet only)

Air Force	
Aircraft Research and Development Unit	1
DGTA	1
Intelligence Program	
DGSTA Defence Intelligence Organisation	1
Information Centre, Defence Intelligence Organisation	1
Corporate Support Program	
OIC TRS, Defence Regional Library, Canberra	1
UNIVERSITIES AND COLLEGES	
Australian Defence Force Academy	1
Library	1
Head of Aerospace and Mechanical Engineering	1
Serials Section (M list), Deakin University Library, Geelong	1
Senior Librarian, Hargrave Library, Monash University	(Doc Data sheet)
Librarian, Flinders University	1
OTHER ORGANISATIONS	
NASA (Canberra)	1
AusInfo	1
OUTSIDE AUSTRALIA	
ABSTRACTING AND INFORMATION ORGANISATIONS	
Library, Chemical Abstracts Reference Service	1
Engineering Societies Library, US	1
Materials Information, Cambridge Scientific Abstracts, US	1
Documents Librarian, The Center for Research Libraries, US	1
INFORMATION EXCHANGE AGREEMENT PARTNERS	
Acquisitions Unit, Science Reference and Information Service, UK	1
Library - Exchange Desk, National Institute of Standards and Technology, US	1
National Aerospace Laboratory, Japan	1
National Aerospace Laboratory, Netherlands	1
SPARES	5
Total number of copies:	**51**

DEFENCE SCIENCE AND TECHNOLOGY ORGANISATION
DOCUMENT CONTROL DATA

1. PRIVACY MARKING/CAVEAT (OF DOCUMENT)

2. TITLE	3. SECURITY CLASSIFICATION (FOR UNCLASSIFIED REPORTS THAT ARE LIMITED RELEASE USE (L) NEXT TO DOCUMENT CLASSIFICATION)
Prediction of Buffet Loads Using Artificial Neural Networks	Document (U) Title (U) Abstract (U)

4. AUTHOR(S)	5. CORPORATE AUTHOR
Oleg Levinski	Aeronautical and Maritime Research Laboratory 506 Lorimer St Fishermans Bend Victoria 3207 Australia

6a. DSTO NUMBER	6b. AR NUMBER	6c. TYPE OF REPORT	7. DOCUMENT DATE
DSTO-RR-0218	AR-012-019	Research Report	September 2001

8. FILE NUMBER	9. TASK NUMBER	10. TASK SPONSOR	11. NO. OF PAGES	12. NO. OF REFERENCES
M1/9/1412	AIR00/142	CDR ARDU	38	22

13. URL on the World Wide	14. RELEASE AUTHORITY
http://www.dsto.defence.gov.au/corporate/reports/DSTO-RR-0218.pdf	Chief, Airframes and Engines Division

15. SECONDARY RELEASE STATEMENT OF THIS DOCUMENT

Approved for public release

OVERSEAS ENQUIRIES OUTSIDE STATED LIMITATIONS SHOULD BE REFERRED THROUGH DOCUMENT EXCHANGE, PO BOX 1500, SALISBURY, SA 5108

16. DELIBERATE ANNOUNCEMENT

No Limitations

17. CASUAL ANNOUNCEMENT Yes

18. DEFTEST DESCRIPTORS

buffeting, Neural networks, Aft fuselages, Tail assemblies, F/A-18 aircraft, Airframes, International Follow On Structural Test Project

19. ABSTRACT

The use of artificial neural networks (ANN) for predicting the empennage buffet pressures as a function of aircraft state has been investigated. The buffet loads prediction method which is developed depends on experimental data to train the ANN algorithm and is able to expand its knowledge base with additional data. The study confirmed that neural networks have a great potential as a method for modelling buffet data. The ability of neural networks to accurately predict magnitude and spectral content of unsteady buffet pressures was demonstrated. Based on the ANN methodology investigated, a buffet prediction system can be developed to characterise the F/A-18 vertical tail buffet environment at different flight conditions. It will allow better understanding and more efficient alleviation of the empennage buffeting problem .